Breakdown of a Space Charge Limited Regime of a Sheath in a Weakly Collisional Plasma Bounded by Walls with Secondary Electron Emission

D. Sydorenko,[1,][*] I. Kaganovich,[2] Y. Raitses,[2] and A. Smolyakov[1]

[1]*Department of Physics and Engineering Physics, University of Saskatchewan, Saskatoon, Saskatchewan S7N 5E2, Canada*
[2]*Princeton Plasma Physics Laboratory, Princeton University, Princeton, New Jersey 08543, USA*

A new regime of plasma-wall interaction is identified in particle-in-cell simulations of a hot plasma bounded by walls with secondary electron emission. Such a plasma has a strongly non-Maxwellian electron velocity distribution function and consists of bulk plasma electrons and beams of secondary electrons. In the new regime, the plasma sheath is not in a steady space charge limited state even though the secondary electron emission produced by the plasma bulk electrons is so intense that the corresponding partial emission coefficient exceeds unity. Instead, the plasma-sheath system performs relaxation oscillations by switching quasiperiodically between the space charge limited and non-space-charge limited states.

A wall immersed in a plasma may emit electrons due to thermionic, field emission, secondary electron, or ion-induced emission, etc. There is a thin non-neutral sheath region at the plasma-wall interface [1], where plasma electrons are reflected by an intense electric field. The emission reduces the sheath electric field, weakening insulation properties of the sheath and enhancing plasma-wall losses [2]. The stronger the emission, the more important is this effect. If the emission intensity increases and approaches some threshold, the wall losses increase drastically and, eventually, the sheath enters a so-called space charge limited (SCL) regime. In this regime, a significant negative charge is accumulated near the wall, which produces a nonmonotonic potential profile in the sheath and returns a part of the emitted electrons back to the wall. The potential drop across the SCL sheath is much lower than that near a non-emitting wall, and the plasma electron flux to the wall is so intense that it can cause evaporation of the wall material. This is particularly important for divertors [3], dusty plasmas [4], Hall thrusters [5], emissive probes [6], etc.

In case of a wall with the secondary electron emission (SEE), the emission intensity is characterized by the emission coefficient γ defined as a ratio of emitted (secondary) and incoming (primary) electron fluxes. If a plasma can be described by a Maxwellian electron velocity distribution function (EVDF), the average emission coefficient can be reduced to a function of the plasma electron temperature. For such a plasma, the SCL sheath regime occurs if the emission coefficient reaches some threshold value $\gamma_{cr} \approx 1$, which is attained at the critical electron temperature T_{cr} [2]. Because of extremely high wall losses in the SCL regime, this critical temperature becomes a virtual upper limit for the electron temperature provided the EVDF is Maxwellian.

This traditional concept based on a Maxwellian EVDF is suitable only for highly collisional plasma systems. It fails for plasmas where the electron energy relaxation length is comparable with or larger than the system size, which is revealed in a number of experimental studies [7–10]. The authors carried out an extensive numerical study of weakly collisional plasmas in Hall thrusters and found that the EVDF in such plasmas is non-Maxwellian, strongly anisotropic, depleted at high energies, and even nonmonotonic [11,12]. The average kinetic energy of a majority of electrons, which are confined by the sheath potential barrier (below they are referred to as the plasma bulk electrons), is several times larger than that in the direction normal to the walls. The plasma bulk electrons reach the walls mostly after scattering off neutral atoms. These collisions are so rare that secondary electrons emitted by the walls propagate through the plasma almost freely, without energy exchange with the plasma electrons. Thus, a wall is bombarded by both the scattered plasma bulk electrons and the electrons emitted from the opposite wall [13]. It appears that while the plasma is heated and the SEE intensity increases, the balance of electron and ion fluxes to the wall is maintained not through the formation of a double layer in the sheath, but through the modification of the EVDF of the plasma-beam system. This new balance mechanism creates an unusual situation in which the SCL sheath practically never develops.

Consider an emitting wall in a bounded weakly collisional plasma. The total primary electron flux to the wall is $\Gamma_1 = \Gamma_{1,p} + \Gamma_{1,b}$, where $\Gamma_{1;p,b}$ are the primary electron fluxes due to the scattered energetic plasma bulk electrons (subscript p) and the beam of secondary electrons (subscript b). This beam can be either emitted from the opposite wall or, if that wall is non-emitting, it can be reflected off the high potential barrier near the non-emitting wall. The total secondary electron flux emitted by the wall is $\Gamma_2 = \Gamma_{2,p} + \Gamma_{2,b}$, where $\Gamma_{2;p,b}$ are the secondary electron fluxes produced by the plasma bulk and secondary beam electrons, respectively. If the secondary electrons propa-

gate freely, then $\Gamma_2 = \Gamma_{1,b}$ and the total emission coefficient is $\gamma \equiv \Gamma_2/\Gamma_1 = \gamma_p/(1 + \gamma_p - \gamma_b)$, where $\gamma_{p,b} = \Gamma_{2;p,b}/\Gamma_{1;p,b}$ are the partial emission coefficients for the aforementioned components [13,14]. The SCL regime establishes when $\gamma > \gamma_{cr}$, which requires

$$\gamma_p > \gamma_{cr}(1 - \gamma_b)/(1 - \gamma_{cr}). \qquad (1)$$

In addition, γ_p cannot exceed the maximum γ_{max} of the curve "emission coefficient versus the energy of primary electrons." Such a curve describes SEE properties of a material. The maximum γ_{max} and the corresponding primary electron energy depend on the material [15]. Condition (1) can be satisfied for $\gamma_p < \gamma_{max}$ provided

$$\gamma_b > 1 - (\gamma_{max}/\gamma_{cr})(1 - \gamma_{cr}). \qquad (2)$$

If the beam energy is low and (2) is not satisfied, the SCL sheath does not appear no matter how big is the plasma bulk electron energy. Note, γ_{cr} corresponds to the SEE intensity at which the secondary electron space charge sets the sheath electric field near the wall to zero. The charge density profile in the sheath, and the γ_{cr}, depend on the EVDF of the plasma and emitted electrons. For qualitative estimates with (1) and (2), one can use γ_{cr} of a plasma with a Maxwellian EVDF [2].

If the secondary electron beam energy ensures (2), and the heating of the plasma is strong, one can expect that the SCL sheath will eventually appear once criterion (1) is satisfied. However, simulation reveals that even in this case, the SCL sheath regime does not become a steady state. Instead, an instability related with a negative differential conductivity of the sheath layer appears [8,16], and a new regime with relaxation oscillations of the sheath between SCL and non-SCL states is observed. This regime is described in the present Letter.

The relaxation oscillations are obtained in electrostatic particle-in-cell (PIC) simulations of a plasma slab bounded by dielectric walls with SEE (see Fig. 1). The PIC code [11,14], based on the direct implicit algorithm [17], resolves one spatial coordinate and three velocity components for the electrons, the ion motion is normal to the walls. The SEE properties approximate that of boron-nitride ceramics [18]. The electron temperature is sustained by crossed constant external electric and magnetic fields. Electrons perform elastic and inelastic (ionization and excitation) collisions with neutral atoms of constant density. The anomalous electron transport across the mag-
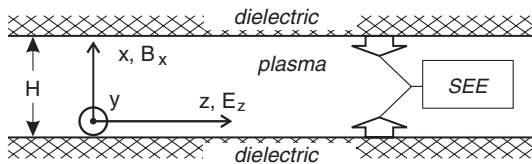
netic field [19,20] is included via the additional "turbulent" collisions, which randomly scatter electrons in the plane parallel to the walls [21].

A representative simulation discussed below is carried out with the parameters typical to Hall thrusters [10]: the external electric field $E_z = 200$ V/cm, the distance between the walls $H = 2.5$ cm, the magnetic field $B_x = 100$ Gauss, the xenon neutral gas density $n_a = 10^{18}$ m^{-3}, the initial plasma density $n_{e0} = 10^{17}$ m^{-3}. In order to demonstrate the SCL regime, the electron heating is enhanced by the increased turbulent collisions frequency $\nu_t = 2.8 \times 10^6$ s^{-1}. The simulation area $0 < x < H$ is divided into 1903 cells, the initial number of electron and ion macroparticles is about 1.9×10^6.

The simulation reveals short periods when the emission coefficient exceeds γ_{cr} [Fig. 2(a)], the primary electron flux to the wall more then doubles [Fig. 2(b)], and the plasma potential relative to the walls drops by a few Volts [Fig. 2(c)]. This is an SCL state with a nonmonotonic potential profile in the sheath (curve 1 in Fig. 3). Every SCL state in Fig. 2 is followed by a much longer non-SCL state, with $\gamma < \gamma_{cr}$ and a monotonic potential profile in the sheath (curve 2 in Fig. 3). Below, the observed global oscillations of the plasma parameters are referred to as the relaxation sheath oscillations (RSO). A distinctive
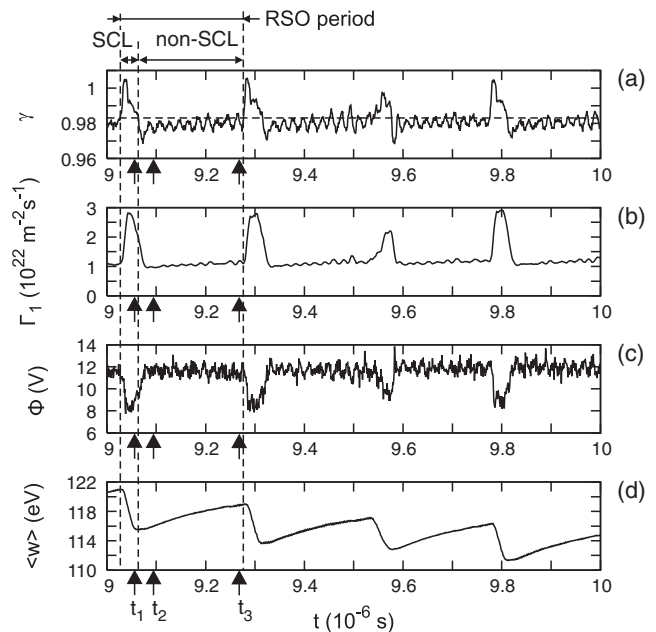
FIG. 2.   Relaxation sheath oscillations. Temporal evolution of emission coefficient at $x = H$ (a), primary electron flux at $x = H$ (b), plasma potential at $x = H/2$ (c), and energy of an electron averaged over all particles (d). Dashed vertical lines mark the beginning and the end of the RSO period and the transition from SCL to non-SCL state. Arrows mark times $t_1 = 9057$ ns, $t_2 = 9095$ ns, and $t_3 = 9269$ ns when the EVDFs shown in Fig. 4 are taken. Dashed horizontal line in (a) marks a theoretical value of the critical emission coefficient $\gamma_{cr} = 0.983$ for a xenon plasma with a Maxwellian EVDF [2].

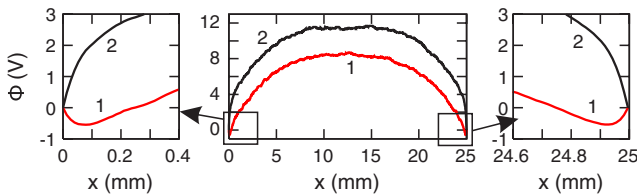FIG. 1.   Schematic diagram of the simulation model. Positions of the walls are $x = 0$ and $x = H$.

FIG. 3 (color online). Typical profiles of plasma potential during the SCL (curve 1, red) and the non-SCL (curve 2, black) regimes. The left and right panels show details of the middle panel in the near-wall regions. The walls are at $x = 0$ and $x = 25$ mm. Curve 1 (red) is at $t = 9038$ ns; curve 2 (black) is at $t = 9076$ ns.

signature of the RSO is the sawtooth curve "the average electron energy versus time" [Fig. 2(d)], where abrupt drops during SCL states (cooling) are followed by gradual increases during non-SCL states (heating).

The reason for the RSO is the non-Maxwellian EVDF. Figure 4 shows EVDFs at three key times of a RSO period (marked by arrows in Fig. 2). The EVDF changes most dramatically for $e\Phi_{SCL} < w_x < e\Phi_{non-SCL}$, where $w_x = mv_x^2/2$ is the energy of electron motion normal to the walls, Φ_{SCL} and $\Phi_{non-SCL}$ are the plasma potential in the midplane relative to the walls during the SCL and non-SCL states. Henceforth, this region in the electron velocity space is called the weakly confined electrons (WCE) area. In Fig. 4, it is bounded by the two vertical dashed lines.

The present model distinguishes two major electron populations: the plasma bulk electrons trapped by the plasma potential and the secondary electron beams freely propagating between the walls. By the end of a non-SCL state, the WCE area of the plasma bulk EVDF contains many electrons with the energy of motion parallel to the walls $w_y + w_z = m(v_y^2 + v_z^2)/2$ big enough to produce SEE with $\gamma > \gamma_{cr}$ [see Figs. 4(c) and 4(f)]. When the plasma potential decreases at the beginning of the SCL state, energetic electrons from the WCE area escape to the walls, producing intense secondary electrons beams [Fig. 4(a)]. Meanwhile, the WCE area becomes empty [see the area between the dashed lines in Fig. 4(d)].

When the intense secondary electron beams with relatively low energy reach the walls, the emission coefficient drops below γ_{cr}, and the plasma potential rises to $\Phi_{non-SCL}$. This happens much faster than the flight time of an electron between the walls. A large number of secondary electrons become trapped by the plasma potential and thus become a part of the plasma bulk [see spikes formed by the trapped electrons in Fig. 4(b)]. The WCE area of the plasma bulk EVDF becomes populated mostly by low-energetic former secondary electrons and depleted of electrons with large transverse energy [see the depleted areas inside the ovals in Fig. 4(e)].

During the non-SCL state, the anisotropic heating by the turbulent collisions replenishes the depleted parts of the WCE area [compare Figs. 4(e) and 4(f)]. This process can
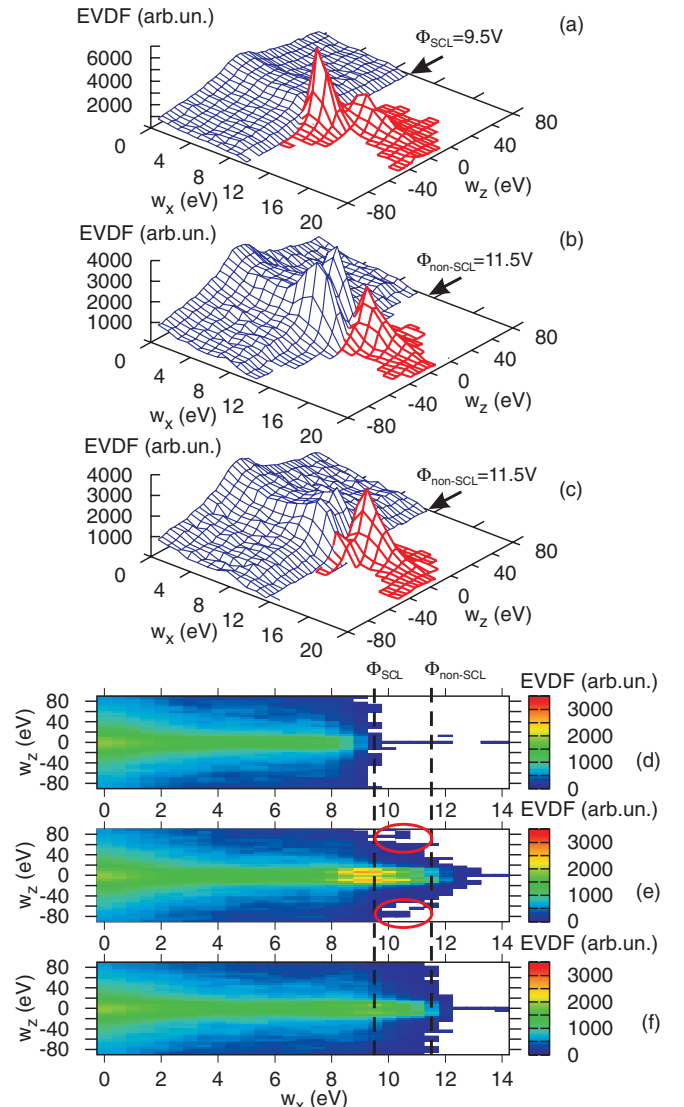

FIG. 4 (color online). EVDFs over v_x and v_z in the middle of the plasma 10 mm $< x <$ 15 mm obtained (a), (d) in the SCL stage at $t_1 = 9057$ ns, (b), (e) in the beginning of the non-SCL stage at $t_2 = 9095$ ns, and (c), (f) in the end of the non-SCL stage at $t_3 = 9269$ ns (times $t_{1,2,3}$ are marked by arrows in Fig. 2). Surfaces depicted by thin (blue) and bold (red) lines in (a), (b), (c) correspond to the electrons of the plasma bulk and the secondary electron beam, respectively. Panels (d), (e), (f) are the color maps of the plasma bulk EVDFs corresponding to the thin-line (blue) surfaces in (a,b,c), respectively. White areas in (d), (e), (f) contain no particles. Ovals in (e) mark areas which are replenished during the non-SCL stage. Graphs are plotted in energy coordinates, negative energy values correspond to propagation in the negative direction. Only parts of EVDFs moving in the positive x direction are shown.

be monitored by the evolution of the curve "average energy of motion in the y-z plane versus the energy of motion normal to the walls," shown in Fig. 5(a). By the end of the non-SCL state, the energy of the weakly confined
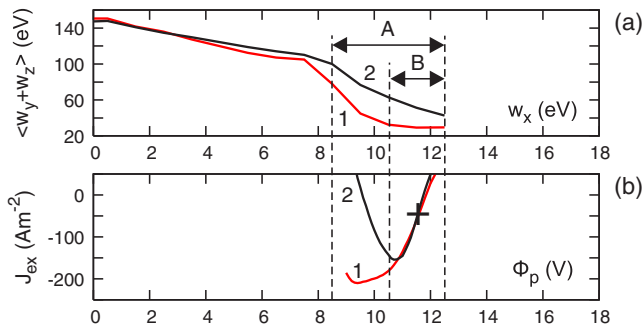
FIG. 5 (color online).   (a) Average energy of motion of plasma bulk electrons in the direction parallel to the walls versus the energy of motion normal to the walls. The dependencies are obtained by averaging over particles in the middle of the plasma $10 \text{ mm} < x < 15 \text{ mm}$. Region A corresponds to electrons escaping to walls during the SCL stage (the weakly confined electrons). Region B corresponds to the range of perturbations of the plasma potential in the system. (b) Total electron current at the wall $x = H$ versus the plasma potential relative to the wall. The cross marks the actual average values of current $J_e \approx -33.3 \text{ A/m}^2$ and potential $\Phi_p \approx 11.5 \text{ V}$ between times t_2 and t_3. Curves 1 (red) are at $t_2 = 9095$ ns, curves 2 (black) are at $t_3 = 9269$ ns (same as $t_{2,3}$ in Figs. 2 and 4).

electrons grows by about 20–30 eV [compare curves 1 and 2 in the region A in Fig. 5(a)].

Because of the energy increase, the weakly confined electrons may produce SEE with $\gamma > \gamma_{cr}$, provided the plasma potential drops and allows them to reach the wall. The current-voltage characteristics of the sheath acquires an unstable branch with the negative differential conductivity [see Fig. 5(b)]. Once the unstable branch appears within the range of plasma potential perturbations, a jump-like transition to the SCL regime occurs, and the process repeats itself. Note, in Fig. 5(b), the unstable branch of curve 2 overlaps with the plasma potential perturbations region B.

In summary, the sheath in a weakly collisional bounded plasma never reaches a steady SCL state even if the plasma bulk electron energy is many times the critical temperature of a plasma with a Maxwellian EVDF (such plasmas are observed in experiments [10]). Instead, the plasma-sheath system performs relaxation oscillations. The oscillation cycle starts with the sheath collapse due to the instability related with the negative differential conductivity of the sheath—the plasma potential decreases, energetic electrons escape to the walls, and the sheath enters the SCL regime. Once a wall encounters an intense flux of cold electrons from the opposite wall, the SCL regime quenches, the high plasma potential restores, and a large number of cold secondary electrons become trapped inside the plasma. Then, these electrons are heated until the sheath becomes unstable again.

The RSO occurs if, first, the secondary electron beam energy at the moment of its impact with the wall is large enough to satisfy (2). The impact energy may exceed the initial emission energy in certain conditions. In Hall thrusters, the additional energy is associated with the drift in crossed electric and magnetic fields [22]. If this drift is slow, the RSO regime does not appear. Second, the heating must be intense and anisotropic. The anisotropy allows accumulation of energetic weakly confined electrons responsible for the negative conductivity. Simulations do not reveal RSO if the turbulent scattering is isotropic. Reduction of the anisotropic scattering frequency ν_t increases the RSO period, and eventually, cancels the RSO regime due to the insufficient heating rate.

*At present time, D. Sydorenko is at the University of Alberta, Edmonton T6G 2G7, Canada.
[1] I. Langmuir, Phys. Rev. **33**, 954 (1929).
[2] G. D. Hobbs and J. A. Wesson, Plasma Phys. **9**, 85 (1967).
[3] S. Takamura, N. Ohno, M. Y. Ye, and T. Kuwabara, Contrib. Plasma Phys. **44**, 126 (2004).
[4] G. L. G. L. Delzanno and M. Rosenberg, Phys. Rev. Lett. **92**, 035002 (2004).
[5] A. I. Morozov, Plasma Phys. Rep. **29**, 235 (2003).
[6] N. Hershkowitz, Phys. Plasmas **12**, 055502 (2005).
[7] R. L. Stenzel, Phys. Rev. Lett. **60**, 704 (1988).
[8] M. C. Griskey and R. L. Stenzel, Phys. Rev. Lett. **82**, 556 (1999).
[9] V. I. Demidov, C. A. DeJoseph, and A. A. Kudryavtsev, Phys. Rev. Lett. **95**, 215002 (2005).
[10] Y. Raitses, D. Staack, M. Keidar, and N. J. Fisch, Phys. Plasmas **12**, 057104 (2005).
[11] D. Sydorenko, A. Smolyakov, I. Kaganovich, and Y. Raitses, IEEE Trans. Plasma Sci. **34**, 815 (2006).
[12] I. Kaganovich, Y. Raitses, D. Sydorenko, and A. Smolyakov, Phys. Plasmas **14**, 057104 (2007).
[13] E. Ahedo and F. I. Parra, Phys. Plasmas **12**, 073503 (2005).
[14] D. Sydorenko, A. Smolyakov, I. Kaganovich, and Y. Raitses, Phys. Plasmas **13**, 014501 (2006).
[15] P. H. Dawson, J. Appl. Phys. **37**, 3644 (1966).
[16] M. Starodubtsev et al., Phys. Rev. Lett. **92**, 045003 (2004).
[17] M. R. Gibbons and D. W. Hewett, J. Comput. Phys. **120**, 231 (1995).
[18] A. Dunaevsky, Y. Raitses, and N. J. Fisch, Phys. Plasmas **10**, 2574 (2003).
[19] G. S. Janes and R. S. Lowder, Phys. Fluids **9**, 1115 (1966).
[20] J. C. Adam et al., Plasma Phys. Controlled Fusion **50**, 124041 (2008).
[21] A. Smirnov, Y. Raitses, and N. Fisch, Phys. Plasmas **11**, 4922 (2004).
[22] In the simulation above, the drift energy contribution $m_e(E_z/B_x)^2/e \approx 23$ eV results in $\gamma_b \approx 0.955$. For $\gamma_{max} = 3$ and $\gamma_{cr} = 0.983$, condition (2) is $\gamma_b > 0.949$.